

Calcite Scale Inhibition Using Environmental-Friendly Amino Acid Inhibitors: DFT Investigation

Rem Jalab, Mohammed A. Saad,* Ibnelwaleed A. Hussein,* and Abdulmujeeb T. Onawole

Cite This: *ACS Omega* 2021, 6, 32120–32132

Read Online

ACCESS |



Metrics & More

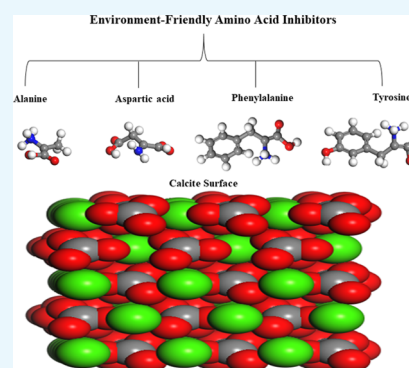


Article Recommendations



Supporting Information

ABSTRACT: Scale prevention is a long-term challenge. It is essential for ensuring the optimum utilization of oil and gas wells and minimizing economic losses due to disruptions in the hydrocarbon flow. Among the commonly precipitated scales is calcite, especially in oilfield production facilities. Previous studies on scale inhibitors have focused on investigating the performance of several phosphonates and carboxylates. However, the increased environmental awareness has pushed toward investigating environmental-friendly inhibitors. Research studies demonstrated the potential of using amino acids as standalone inhibitors or as inhibitor-modifying reagents. In this study, 10 amino acids for calcite inhibitors have been investigated using molecular simulations. Eco-toxicity, quantum chemical calculations, binding energy, geometrical, and charge analyses were all evaluated to gain a holistic view of the behavior and interaction of these inhibitors with the calcite {1 0 4} surface. According to the DFT simulation, alanine, aspartic acid, phenylalanine, and tyrosine amino acids have the best inhibitor features. The results revealed that the binding energies were -2.16 , -1.75 , -2.24 , and -2.66 eV for alanine, aspartic acid, phenylalanine, and tyrosine, respectively. Therefore, this study predicted an inhibition efficiency of the order tyrosine > phenylalanine > alanine > aspartic acid. The predicted inhibition efficiency order reveals agreement with the reported experimental results. Finally, the geometrical and charge analyses illustrated that the adsorption onto calcite is physisorption in the acquired adsorption energy range.



1. INTRODUCTION

Oilfield scales are mostly inorganic salts deposited by precipitation at the conditions of water supersaturation. These mineral salts in the water remain dissolved in undersaturation conditions and start precipitating when the conditions change to supersaturation.¹ Scales deposits are impervious and form a precipitate layer on solid surfaces, causing problems in oil and gas flow assurance. Consequently, the scales could result in depleted hydrocarbons production and equipment obstruction, leading to economic losses and costly shutdown of facilities. It was estimated that the nonproductive shutdown expenses reached 3 billion and 9 billion USD in Japan and the USA, respectively.² Therefore, to avoid detrimental impacts on oil and gas exploitation, it is quite important to understand the scale formation mechanisms and its prevention approaches.

Scale formation encompasses sophisticated surface and bulk crystallization phenomena.³ Crystallization and precipitation of scales are realized when the ions are above their saturation level. Considering the precipitation kinetics enables the determination of scaling severity. Thereafter, when the supersaturation condition reaches a critical limit, the nucleation of scale formation prompts the crystal growth, and crystallization kinetics decelerate due to low nucleation sites.⁴ Generally, the scale formation steps comprise aggregation, nucleation, crystal growth, and agglomeration.⁵ Scale formation is influenced by many operating conditions,

including temperature,⁶ operating pressure,¹ pH, and flow velocity.⁷ Other factors that could enhance the scaling tendency are high concentration minerals, the roughness of the surface, and incompatible mixing of formation water and injected water.⁸

The different types of scales in oilfields involve carbonates, sulfides, sulfates, alumina silicates, and phosphates.^{9,10} Calcium carbonate has been reported as the most encountered scale in the upper sections of the production facilities and the production piping in the oilfield.¹¹ The colloidal and amorphous states of calcium carbonate appear in three different forms, namely, calcite, aragonite, and vaterite.¹² Calcite is the most stable form at the reservoir conditions, hence the most widespread.¹⁰ Under the actions of low CO₂ partial pressure and high temperature, the soluble calcium bicarbonate in water is transformed into the less soluble calcium carbonate, resulting in the formation of calcite deposits (eq 1).¹³ Despite the effect of pressure and temperature, the

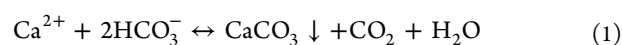
Received: September 5, 2021

Accepted: October 29, 2021

Published: November 16, 2021



formation of calcite is a function of pH, ionic strength, and bicarbonate and calcium concentrations.



Calcite deposits removal is relatively unchallenging since it is pH-dependent. Thus, dilute HCl acid can be easily applied for its treatment. Despite applying acid cleaning for the removal of the existing scales, scale inhibitors (SIs) are usually used for disrupting the calcite film formation.

Scale inhibitors are chemical compounds capable of preventing precipitation, deposition, and growth on solid surfaces. For instance, phosphate esters and phosphonates, such as diethylenetriamine pentamethylene phosphonic acid (DTPMP), are very efficient for the inhibition of calcite scales.¹⁴ The effective polymeric and nonpolymeric SIs used in the oilfield are organic phosphonates, sulfonates, and carboxylates containing $-\text{PO}_3\text{H}_2$, $-\text{SO}_3\text{H}$, and $-\text{COOH}$, respectively.¹⁵ Furthermore, some polymeric inhibitors of polyacrylates, polyphosphino carboxylates, polymaleates, and polyacrylamides are adequately stable at high temperatures reaching 200 °C; making them suitable and effective for calcite formation inhibition in oil reservoirs.¹⁶ Most of the reported studies focus on investigating the performance of several phosphonates and carboxylates inhibitors due to their outstanding efficiency in the oilfield.^{17–21} In spite of the good inhibition performance, those inhibitors are not classified as environmental-friendly because they possess a degree of toxicity. The increased environmental awareness and strict regulations have pushed toward investigating environmental-friendly inhibitors either by modifying the structures of the state-of-the-art inhibitors²² or by proposing new green ones.^{23–25}

Green inhibitors (GIs) are biodegradable, nontoxic, and sometimes nitrogen-free or phosphorus-free compounds with relatively high efficiency.²⁶ They have the capabilities of preventing calcite formation in an aqueous medium through the dispersion and aqua-complexation actions, along with the possibility of inhibiting the growth at the solid–liquid interfaces.^{26,27} Several plant extracts have been used as natural organic antiscalants, relying on their easy extraction and built-in ion complexing functional groups.²⁸ *Raphanus sativus* L. ethanol and *Gypsophila aretioides* roots have shown successful prevention of calcite precipitation.^{29,30} Furthermore, new polymeric reagents based on the polyacrylates are developed through the integration of several monomer fragments for enhanced biodegradability.³¹

Nevertheless, it was stated that the two most efficient synthetically prepared green inhibitors from petrochemicals are mainly polyaspartic acid (PASP) and polyepoxysuccinic acid (PESA).³² Despite the excellent performance of both inhibitors for calcite scale control, PESA showed better performance than PASP and recorded 90% inhibition efficiency.^{31,33} However, the modification of these antiscalants by introducing different functional groups to the polymer chain has become a research hotspot for the improvement of their performance and environmental impacts. A polymer prepared from epoxysuccinic acid (ESA), itaconic acid (IA), and sodium methyl propylene sulfonate (SMAS) exhibited an inhibition efficiency reaching 100% with good biodegradability.³⁴ Additionally, modifications of PASP are also examined to boost its poor performance observed at high temperatures.³⁵ A research study presented the modification of PASP by adding two different environmental-friendly amino acids to the side chains; since

carboxylic acid groups showed promising performance in industrial applications.³⁶ Amino acids are among the commonly applied functional groups contributing to the formation of crosslinks with the side chains.

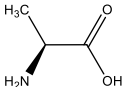
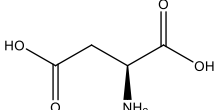
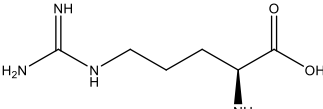
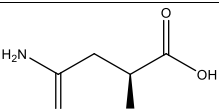
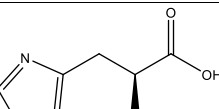
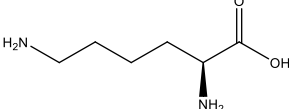
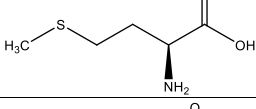
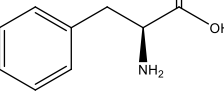
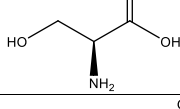
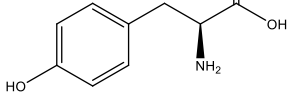
Amino acids are green, abundant, and readily obtainable functional groups at low cost with high purity.^{37,38} Nonetheless, they are featured with the properties of a good scale inhibitor represented by having heteroatoms (N, P, and O) and double bonds facilitating their adsorption onto the surfaces.³⁹ An experimental study examined the effect of seven different amino acids on the precipitation of calcite. The study disclosed the promising influence of amino acids through the interaction with calcite surface.²⁵ However, the studies that examine amino acids for scale inhibition are rare; instead, they have been extensively investigated as corrosion inhibitors against many metal surfaces.^{40–42} Research works demonstrated the promising potential of using amino acids as standalone inhibitors or as reagents to modify inhibitors.^{25,36} Thus, this has encouraged the investigation of the interaction mechanism of amino acid with calcite scale at the molecular level through molecular simulation.

Recently, molecular modeling methods, including density functional theory (DFT), have become a beneficial tool; displacing the time-consuming experimental analysis accompanied by financial and chemical losses.⁴³ These methods enable the preselection of inhibitors, before conducting laboratory analysis, through the prediction of some quantum chemical and electronic structure parameters. Several studies investigating amino acids as corrosion inhibitors have conducted molecular modeling techniques.^{44–46} Few other studies considered specific amino acid molecules as antiscalants and examined the interaction with calcite surface.^{47,48} The literature search shows that theoretical studies illustrating the interaction of these amino acids with calcite are rare. In this study, molecular simulation has been employed to study the performance of 10 selected amino acids for calcite inhibition. First, the assessment of eco-toxicity of all the considered amino acids is performed using a designed web tool. After that, and using DFT, the electronic properties of the amino acid structures are studied at the molecular level. The interaction energy with the calcite surface is determined for the optimum four amino acid molecules relying on the predicted DFT parameters. The calcite {1 0 4} surface was explored for potential adsorption sites that facilitate the interaction with the inhibitors by placing the inhibitors over three different positions (top, middle, and bottom). Lastly, the Bader charge analysis is implemented to gain a holistic insight into the mechanism of interaction of amino acid molecules with calcite and adsorption on it. Overall, the theoretical evaluation provides support for elucidating the performance of environmental-friendly inhibitors and gives guidance for laboratory analysis.

2. MATERIALS

This theoretical study aims to investigate the effect of adding environmental-friendly amino acid inhibitors for the inhibition of calcite scale. The selected amino acids with their structures and properties are listed in Table 1. The use of ACD/ChemSketch software enables the determination of the density of each amino acid molecule at standard temperature (273.15 K) and pressure (1 atm).⁴⁹

Table 1. Properties of Selected Amino Acid Inhibitors

Scale Inhibitor	Chemical Structure	Formula	Mw (g/mol)
Alanine		C ₃ H ₇ NO ₂	89.09
Aspartic Acid		C ₄ H ₇ NO ₄	133.10
Arginine		C ₆ H ₁₄ N ₄ O ₂	174.20
Asparagine		C ₄ H ₈ N ₂ O ₃	132.11
Histidine		C ₆ H ₉ N ₃ O ₂	155.15
Lysine		C ₆ H ₁₄ N ₂ O ₂	146.18
Methionine		C ₅ H ₁₁ NO ₂ S	149.21
Phenylalanine		C ₉ H ₁₁ NO ₂	165.19
Serine		C ₃ H ₇ NO ₃	105.09
Tyrosine		C ₉ H ₁₁ NO ₃	181.19

3. QUANTUM CHEMICAL CALCULATION METHODOLOGY

The computational chemistry studies are based on the density functional theory (DFT) method. All DFT simulations were performed using Gaussian 09 software for the preparation of input files.⁵⁰ The input files were created for the objective of optimizing the amino acid structures and calculating the frequency. The calculations were made using ground-state DFT and Becke 3 Lee, Yang, and Parr (DFT-B3LYP) methods with the 6-31G++ (d,p) basis set. The B3LYP method was chosen as it is one of the robust DFT methods, which gives good accuracy with low computational cost.⁵¹ Hence, its reliability and popularity in the literature, including calcu-

lations involving corrosion inhibitors.^{52,53} On the other hand, the 6-31G++ (d,p) basis set, which is a reasonably large basis set, was employed to minimize basis set errors.⁵⁴ The polarizable continuum model-self-consistent reaction field (PCM-SCRF) was applied for water solvent to represent the real case scenario.⁵⁵ Before running the optimization calculations, it was ensured that the vibration analysis involved no imaginary frequency for guaranteeing optimized structures in the minimum energy state.

After geometry optimization, the output data was utilized for quantum chemical calculations that reflect the activity of amino acid molecules. These electronic structure parameters of each molecule are associated with the energy of the highest occupied molecular orbital (E_{HOMO}) and the lowest unoccupied molecular orbital (E_{LUMO}) obtained from output files. E_{HOMO} indicates the ability of the inhibitor to donate an electron to the unoccupied orbital of another molecule and bind with it.⁴⁴ Koopman's theory states that the ionization energy (I) correlates to $I = -E_{\text{HOMO}}$ and electron affinity to $A = -E_{\text{LUMO}}$.^{56,57} The reactivity indexes comprising electronegativity (χ), chemical hardness (η), and potential (μ) are obtained, relying on the values of I and A (eqs 2–4).^{58,59} After that, the electronegativity index (ω) is found from eq 5. Lastly, the total negative charge (TNC) parameter is found from Mulliken charges to demonstrate the number of adsorption sites on the surface of amino acid molecules.⁶⁰

$$\eta = \frac{I - A}{2} \quad (2)$$

$$\chi = \frac{I + A}{2} \quad (3)$$

$$\mu = -\chi \quad (4)$$

$$\omega = \frac{\mu^2}{2\eta} \quad (5)$$

The Vienna ab initio simulation package (VASP) version 5.4.4 code was used for performing the periodic DFT calculations for the best four amino acid inhibitors based on the analysis of the results of preliminary DFT parameters (quantum chemical parameters).⁶¹ Periodic boundary conditions (PBCs) were applied for the four systems to enable the approximation of a real large-scale system on a small-scale unit cell. For the exchange–correlation energy of elements, the revised generalized gradient approximation of Perdew, Burke, and Ernzerhof (PBE-GGA) was used instead of local density approximation (LDA) for providing better equilibrium structural parameters.^{62,63} Periodic DFT calculations are useful for determining the interaction energies between the inhibitors and calcite scale surface. The projected augmented wave (PAW) pseudopotentials were used to describe the interactions of ions and electrons.^{64,65} Through the performed calculations, the semi-empirical correction by Grimme (DFT + D3) was employed to represent the dispersion forces between the surfaces and interfaces.^{66,67}

Calcite {1 0 4} surface of a hexagonal crystalline structure with the $R\bar{3}c$ space group was obtained from the database in a material studio.⁶⁸ The lattice parameters of the calcite bulk employed in this study were $a = 16.19 \text{ \AA}$, $b = 14.97 \text{ \AA}$, and $c = 25.74 \text{ \AA}$. The calcite interface was extended to five layers containing 300 atoms, with the bottom layer being fixed to represent the nature bulk. The bulk calcite structure was

Table 2. Eco-Toxic Properties of Amino Acid Inhibitors^{74–77}

amino acid compound	carcinogenicity	eye irritation	ames mutagenesis	acute oral toxicity (class III)	honey bee toxicity	crustacean aquatic toxicity	fish aquatic toxicity	water solubility log S (ESOL)
alanine	0.59(safe)	0.69 (toxic)	0.93 (safe)	0.54 (slightly toxic)	0.66 (safe)	0.98 (safe)	0.90 (safe)	1.54 (highly soluble)
aspartic acid	0.83 (safe)	0.64 (toxic)	0.86 (safe)	0.59 (slightly toxic)	0.64 (safe)	0.92 (safe)	0.91 (safe)	1.98 (highly soluble)
arginine	0.91 (safe)	0.95 (safe)	0.63 (safe)	0.64 (safe)	0.78 (safe)	0.88 (safe)	0.97 (safe)	2.12 (highly soluble)
asparagine	0.86 (Safe)	0.66 (toxic)	0.87 (safe)	0.53 (safe)	0.78 (safe)	0.95 (safe)	0.94 (safe)	1.69 (highly soluble)
histidine	0.94 (safe)	0.91 (safe)	0.74 (safe)	0.54 (slightly toxic)	0.72 (safe)	0.73 (safe)	0.94 (safe)	1.30 (highly soluble)
lysine	0.83 (safe)	0.65 (safe)	0.62 (toxic)	0.49 (safe)	0.73 (safe)	0.78 (safe)	0.93 (safe)	1.51 (highly soluble)
methionine	0.79 (safe)	0.95 (safe)	0.88 (safe)	0.62 (safe)	0.59 (safe)	0.71 (safe)	0.83 (safe)	0.68 (highly soluble)
phenylalanine	0.80 (safe)	0.79 (safe)	0.90 (safe)	0.68 (slightly toxic)	0.69 (safe)	0.78 (safe)	0.67 (safe)	−0.08 (very soluble)
serine	0.77 (safe)	0.74 (toxic)	0.92 (safe)	0.51 (slightly toxic)	0.66 (safe)	0.97 (safe)	0.96 (safe)	1.57 (highly soluble)
tyrosine	0.66 (safe)	0.77 (toxic)	0.76 (safe)	0.64 (slightly toxic)	0.55 (safe)	0.78 (safe)	0.59 (safe)	0.39 (highly soluble)

optimized using a plane-wave energy cutoff of 367.69 eV. In addition, a $1 \times 2 \times 1$ *k*-point sampling grid was adopted for the DFT optimization calculations as it achieved the necessary energy convergence in our earlier work,⁶⁹ being computationally efficient compared to the Monkhorst–Pack grid.⁷⁰

Consequently, to calculate the adsorption energies, the optimized amino acid inhibitors were positioned above the optimized calcite surface. The combined systems were created using Quantum ATK visual nano lab software^{71,72} and visualized using Materials Studio.⁷³

Lastly, ADMETSAR 2 program was utilized for the prediction of the eco-toxic properties of each inhibitor.^{74,75} ADMETSAR is a web tool for the assessment of the absorption, distribution, metabolism, excretion, and toxicity (ADMET) properties. This program is based on more than 210 000 experimental findings for around 100 000 through a machine-learning model. SwissADME website,^{76,77} which was created to predict ADME parameters as well the pharmacokinetic properties, was also employed for predicting the solubility of amino acid molecules in water.

4. RESULTS AND DISCUSSION

4.1. Eco-Toxicity Assessment. Prior to investigating the inhibition performance of the aforementioned amino acids, the ecological properties were predicted using ADMETSAR and SwissADME programs.^{74–77} With the aid of that web tool, the interaction of the inhibitors with the environment and humankind was assessed. The main eco-toxic properties focusing on carcinogenicity, eye irritation, biodegradability, aquatic toxicity, and water solubility were predicted for each amino acid, as shown in Table 2. The choice of these descriptors is based on their importance to the environment and living organisms. These descriptors are essential for classifying the environmental-friendly nature of the inhibitors.

Results show that all inhibitors are safe from carcinogenicity, honey bee toxicity, crustacean, and aquatic fish toxicity. For the mutagenic potential of inhibitors measured through the Ames mutagenesis test, all inhibitors are considered safe except lysine, which has a 62% probability of causing mutations in the DNA of the organisms. Asparagine, arginine, lysine, and methionine are safe when considering the acute oral toxicity

(class III), while the remaining inhibitors are slightly toxic with a maximum probability of 68% for phenylalanine. However, acute oral toxicity is not a significant property, assuming it will not be taken orally. Alanine, aspartic acid, serine, and tyrosine possess an eye irritation potential with a maximum probability of 77% for tyrosine.

All inhibitors range from very soluble to highly soluble in water. The predictions using SwissADME are based on the estimated solubility (ESOL), which allows the prediction of aqueous solubility for the molecular structure. The ESOL model is derived from the linear regression of 2874 measured values for the solubility against nine properties.⁷⁸ For this solubility type, any chemical compound is insoluble when $\log S < -10$, poorly soluble when $\log S < -6$, moderately soluble when $\log S < -4$, soluble when $\log S < -2$, very soluble when $\log S < 0$, and highly soluble when $\log S > 0$.⁷⁷ Relying on the water solubility predictions, the solubility of amino acids is of the order arginine > aspartic acid > asparagine > serine > alanine > lysine > histidine > methionine > tyrosine > phenylalanine. The lowest water solubility possessed by phenylalanine and tyrosine could probably be assigned to the presence of the aromatic ring in their molecular structure.⁷⁹

4.2. Quantum Chemical Calculations. The optimization calculations of amino acid inhibitors using the DFT-B3LYP methods have enabled the visualization of optimized molecular structures, electrostatic potential (ESP) maps, highest occupied molecular orbital (HOMO), and lowest unoccupied molecular orbital (LUMO) as shown in Table 3. The ESP maps provide a visual understanding of the electron density variation among the parts of the molecular structure. The colors of ESP maps indicate the extent of the electrostatic potential that possesses ascending order starting from red, orange, yellow, green, and blue regions sequentially.⁸⁰ According to the generated ESP maps (Table 3), blue and red colors dominate most molecular regions. The strong negative electrostatic potential indicated by the red color was mainly observed over the oxygen atoms, whereas the strong positive electrostatic potential represented by the blue color was remarked over amine groups and part of the hydrocarbon chains. In addition, some regions are colored with light green, indicating a zero electrostatic potential.⁴⁴ HOMO and LUMO

Table 3. Optimized Structures of Amino Acid Inhibitors, HOMO, LUMO, and ESP

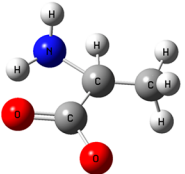
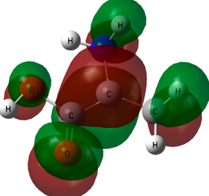
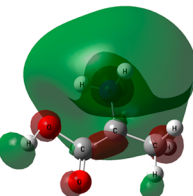
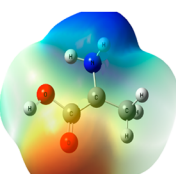
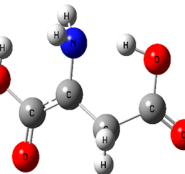
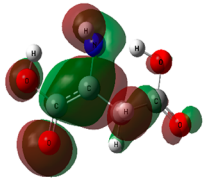
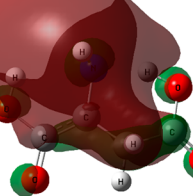
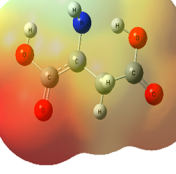
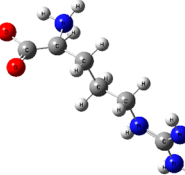
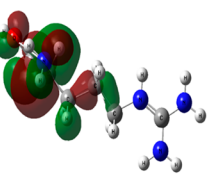
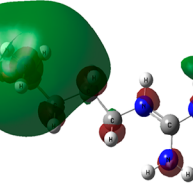
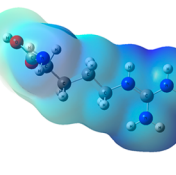
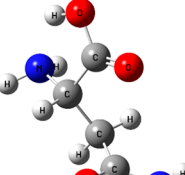
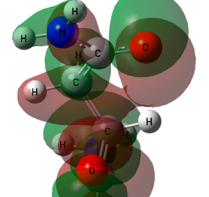
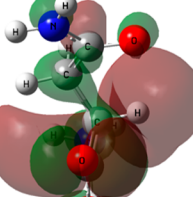
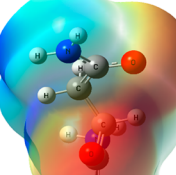
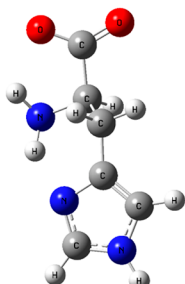
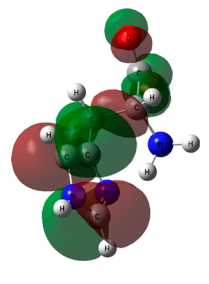
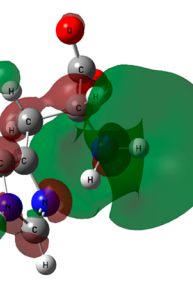
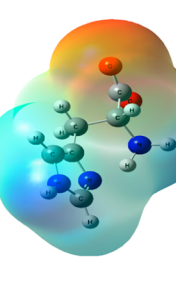
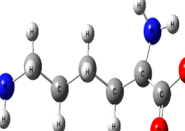
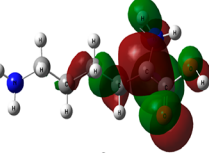
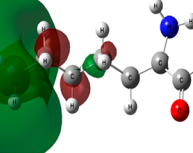
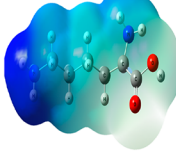
Inhibitor	Optimized structure	HOMO	LUMO	ESP
<i>Alanine</i>				
<i>Aspartic acid</i>				
<i>Arginine</i>				
<i>Asparagine</i>				
<i>Histidine</i>				
<i>Lysine</i>				

Table 3. continued

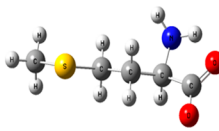
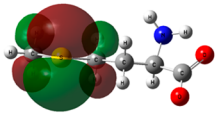
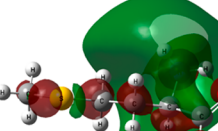
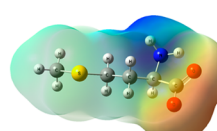
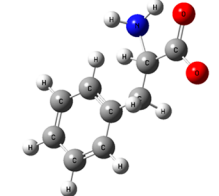
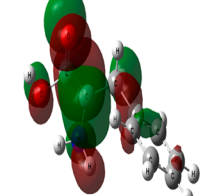
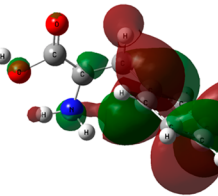
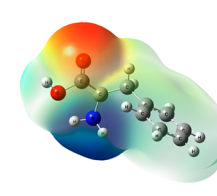
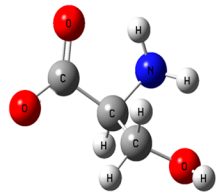
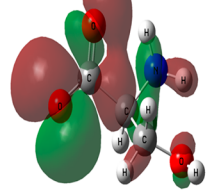
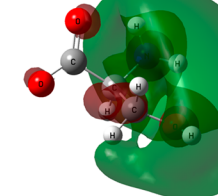
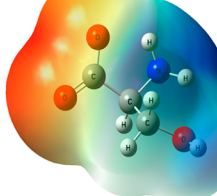
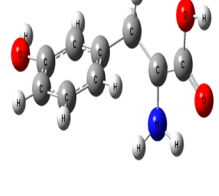
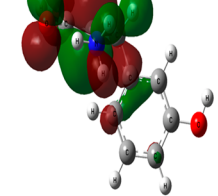
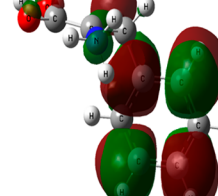
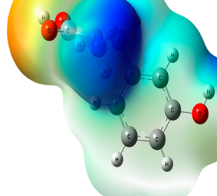
Inhibitor	Optimized structure	HOMO	LUMO	ESP
<i>Methionine</i>				
<i>Phenylalanine</i>				
<i>Serine</i>				
<i>Tyrosine</i>				

Table 4. Quantum Chemical Parameters for Amino Acids Inhibitors

amino acid compound	HOMO (eV)	LUMO (eV)	$\Delta E_{\text{Gap}} (LUMO-HOMO)$ (eV)	I (eV)	A (eV)	η (eV)	X (eV)	ω (eV)	TNC (eV)
alanine	-4.99	-0.51	4.47	4.99	0.51	2.24	2.75	8.46	-2.44
aspartic acid	-4.43	-0.37	4.07	4.43	0.37	2.03	2.40	5.85	-3.40
arginine	-5.13	-0.55	4.57	5.13	0.55	2.29	2.84	9.22	-4.59
asparagine	-7.36	-0.57	6.79	7.36	0.57	3.40	3.97	26.70	-3.53
histidine	-6.60	-0.29	6.31	6.60	0.29	3.15	3.45	18.73	-3.50
lysine	-5.08	-0.65	4.43	5.08	0.65	2.22	2.87	9.11	-3.69
methionine	-6.30	-0.45	5.85	6.30	0.45	2.92	3.38	16.66	-3.68
phenylalanine	-5.09	-0.54	4.55	5.09	0.54	2.27	2.82	9.03	-4.41
serine	-6.97	-0.46	6.51	6.97	0.46	3.26	3.72	22.49	-2.68
tyrosine	-5.12	-0.53	4.59	5.12	0.53	2.29	2.83	9.17	-5.20

representations show atoms with electron-donating and electron-accepting capabilities, respectively.

As explained earlier, quantum chemical parameters are derived from a set of equations from the DFT calculations, which reflect the inhibition performance of each amino acid inhibitor (Table 4). E_{HOMO} and E_{LUMO} values of the inhibitors suggest that aspartic acid and asparagine inhibitors have the highest and lowest electron-donating abilities, respectively, while histidine and lysine have the highest and lowest electron-

accepting abilities, respectively. Referring to Koopman's theory, the inhibitors with the lowest HOMO (asparagine) and LUMO (lysine) have the highest ionization energy and electron affinity of 7.36 and 0.65 eV, respectively. This indicates that better reactivity of inhibitor is achieved when ionization energy is low.⁸⁰ Additionally, the energy gap between HOMO and LUMO ($\Delta E_{\text{Gap}} (LUMO-HOMO)$) is an important parameter for describing the reactivity of inhibitor with the surface. A high energy gap is translated into low

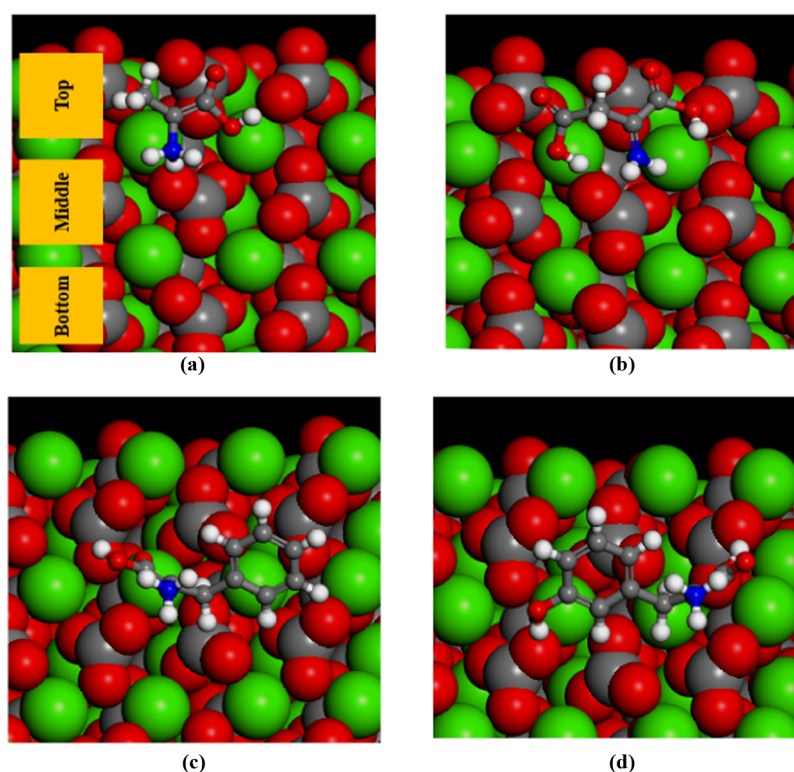


Figure 1. Top view of the optimized structures of the calcite {1 0 4} surface with (a) alanine (on top), (b) aspartic acid (on top), (c) phenylalanine (in middle), and (d) tyrosine (in middle).

inhibition efficiency of the amino acid molecules.⁴⁴ This means that aspartic acid is characterized by having the highest inhibition efficiency (lowest $\Delta E = 4.07$ eV) compared to the other studied amino acid inhibitors. However, asparagine is the molecule with the lowest inhibition efficiency having the highest ΔE of 6.79 eV.

Furthermore, low electronegativity is another feature pointing toward a good inhibitor.⁸⁰ This is in agreement with the obtained results, confirming that aspartic acid has the best inhibition performance with the highest capability to attract a shared pair of electrons. For the measurement of electron attraction reactivity, the electrophilicity index (ω) was considered to predict the energy of molecular stability after attracting those electrons. High and low ω values indicate good electrophilicity and nucleophilicity, respectively.⁸¹ In the case of studied amino acids, the top three electrophiles are aspartic acid, alanine, and phenylalanine with indexes of 5.85, 8.46, and 9.03 eV, respectively. In addition, aspartic acid is the softest inhibitor as observed from the chemical hardness (η) parameter of 2.03 eV. A high hardness refers to low reactivity and difficult transfer of electrons to an acceptor.⁴⁴ Following aspartic acid, lysine is the second soft inhibitor, while asparagine is the last in the order hardness ($\eta = 3.40$ eV). In fact, high TNC implies higher donation of electrons to the unoccupied molecular orbitals of acceptor and stronger adsorption onto the scale surface.^{58,81} Charge distribution marked the highest negative charge for tyrosine inhibitor and lowest for alanine.

Generally, a suitable inhibitor is recognized by having low electronegativity, high TNC, and strong nucleophilicity (low ω).^{44,58,80,81} Relying on the quantum chemical parameter analysis (Table 3), aspartic acid, alanine, phenylalanine, and tyrosine amino acid inhibitors are the top four inhibitors that

comply with the aforementioned criteria. Therefore, these four amino acid molecules are chosen for further examination of their interaction with the calcite scale surface.

4.2.1. Inhibitor-Scale Surface Interaction Energy. Four systems containing the four chosen inhibitors each with a calcite scale slab were built and optimized. Through this study, the calcite surface was explored for potential adsorption sites that facilitate interaction with the inhibitors. Therefore, the inhibitors were placed over three different positions on the calcite surface: top, middle, and bottom (Figure 1). The inhibition efficiency of the amino acid structures was evaluated based on the calculation of adsorption energy (binding energy) found from the below expression

$$\Delta E_{\text{adsorption (binding)}} = E_{\text{surface+inhibitor}} - (E_{\text{surface}} + E_{\text{inhibitor}}) \quad (6)$$

The calculated adsorption energies for the optimum systems are shown in Table 5, with negative values indicating the spontaneous and exothermic nature of the reactions. The interaction energies of surface and inhibitors for the other positions are reported in the Supplementary Information (Table S1). The inhibition performance of the selected amino acid inhibitors is of the order tyrosine (-2.66 eV) >

Table 5. Inhibitor-Scale Surface Interaction Energy

inhibitor	E_{surface} (eV)	$E_{\text{inhibitor}}$ (eV)	$E_{\text{surface+inhibitor}}$ (eV)	$E_{\text{adsorption}}$ (eV)
alanine (top)	-2243.33	-74.18	-2319.68	-2.16
aspartic acid (top)		-92.84	-2337.93	-1.75
phenylalanine (middle)		-143.32	-2388.90	-2.24
tyrosine (middle)		-150.18	-2396.18	-2.66

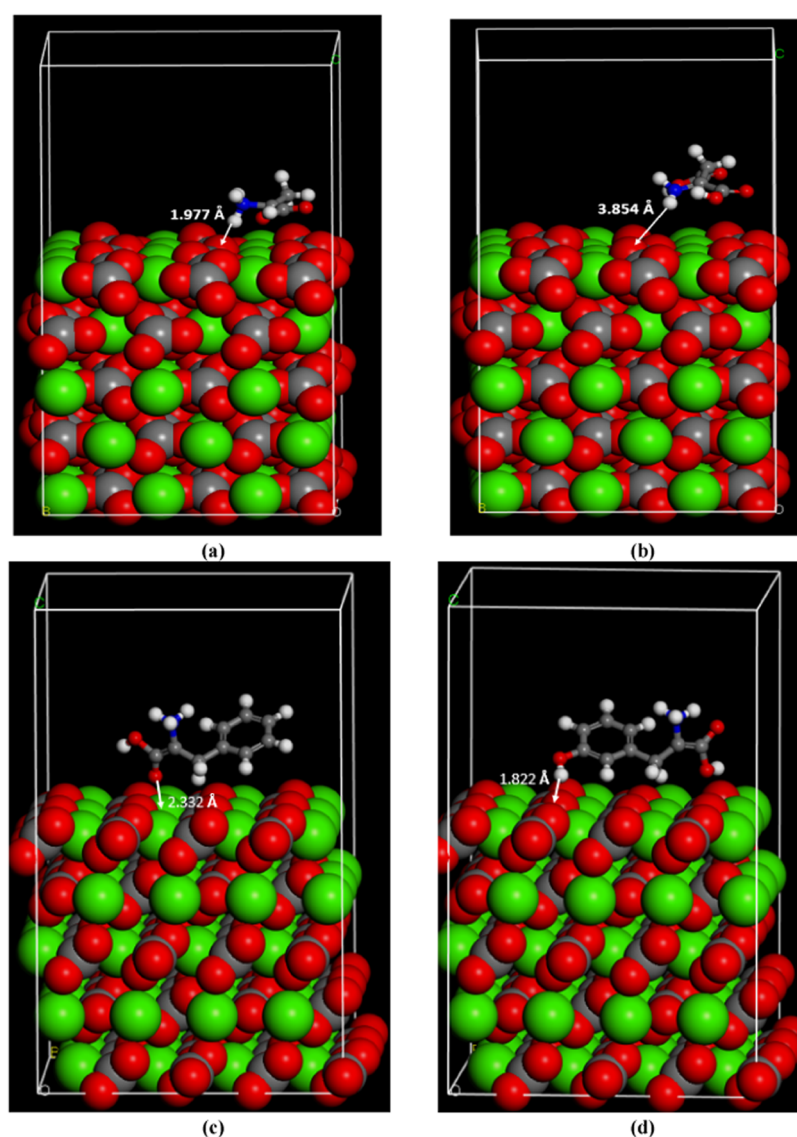


Figure 2. Side view of the optimized structures of the calcite {1 0 4} surface with (a) alanine (on top), (b) aspartic acid (on top), (c) phenylalanine (in middle), and (d) tyrosine (in middle).

phenylalanine (-2.24 eV) > alanine (-2.16 eV) > aspartic acid (-1.75 eV).

Molecular simulation has predicted that tyrosine is the most efficient inhibitor in catching the present calcite scale. In fact, this is translated into realizing that the tyrosine surface has suitable binding locations compared to the other three inhibitors. Additionally, the highest negative value indicated the highest stability of the tyrosine–calcite complex. Phenylalanine and tyrosine inhibitors in the middle position over the calcite surface succeeded in acquiring the highest adsorption energies, owing to their molecular structure containing the aromatic rings. This could suggest that the rings in their structure provide higher calcite surface coverage ability, thus higher binding energy.

To the best of our findings, there is a lack of experimental research work that studies the inhibition efficiency of the exact amino acids considered in the present study with calcite. Hence, for assessing the validity of the predicted inhibition efficiency order, a comparison between results combined from different literature studies was considered. For instance, an experimental study by Štajner et al.²⁵ investigated (alanine,

aspartic acid, phenylalanine, and tyrosine) as charged molecules for determining their effect on calcite precipitation. The study reported that the adsorption of aspartic acid onto the {1 0 4} calcite surface is very weak at low and progressive supersaturation attainment conditions (titration or gas diffusion) during the precipitation experiments.²⁵ Indeed, this observation agrees with the predicted adsorption energies, asserting that aspartic acid possesses the weakest interaction with calcite (Table 5).

Moreover, another experimental work by Hamdona et al.⁸² revealed a higher inhibition efficiency of phenylalanine (17.94%) for calcite than achieved by alanine (13.08%) at the studied conditions. Nonetheless, phenylalanine possessed a distinctly lower inhibition efficiency of (36%) than tyrosine (82%) for the inhibition of copper corrosion.⁸³ Combining all of the experimental findings, we demonstrate an agreement between the predicted inhibition efficiency order of the studied amino acid structures and the theoretical calculations.

Compared with typical commercial-scale inhibitors, including nitrilotriacetic acid (NTA) and ethylenedinitrilotetraacetic acid (EDTA), the studied amino acids exhibit slightly lower

adsorption onto the calcite surface. According to molecular dynamic simulations and quantum calculations by Ji et al.,⁸⁴ the adsorption energies of NTA and EDTA onto the calcite {1 0 4} surface are -3.10 and -2.76 eV, respectively. Tyrosine (-2.66 eV) shows a very close binding energy with the calcite surface compared with EDTA (-2.76 eV). Generally, results reveal trivial differences in adsorption between the two sets of inhibitors (Table 5), with the ones proposed in this study being green inhibitors with low environmental risk. This confirms the potential of these amino acids to successfully replace some of the toxic and nonenvironmental-friendly phosphonate- and carboxylate-based inhibitors.

4.2.2. Geometrical Analysis. The structures of the optimized calcite slab surface with alanine, aspartic acid, phenylalanine, and tyrosine inhibitors are illustrated in Figures 1 and 2. A three-dimensional (3D) analysis of optimized geometrical structures demonstrates the distance and bonds formed between the inhibitor and calcite slab. The shortest distance was observed to occur through O–H and O–Ca bonds with H of O–H and O of O–Ca from the scale inhibitor and O of O–H and Ca of O–Ca from the calcite slab. The shortest measured lengths between the closest heteroatoms are reported in Table 6.

Table 6. Shortest Distance between Calcite Slab and the Inhibitors

inhibitor	shortest distance (Å)	bond type
alanine (on top)	1.98	O–H
aspartic acid (on top)	3.85	O–H
phenylalanine (in middle)	2.33	Ca–O
tyrosine (in middle)	1.82	O–H

4.2.3. Charge Analysis. The Bader charge analysis related to determining the charge distribution of each inhibitor before and after the interaction with the calcite surface was performed. This charge analysis is essential for further understanding the nature of inhibitor adsorption and the perception of the inhibitor–calcite surface interaction mechanism. The charge densities of the four inhibitors in the optimum positions over the calcite {1 0 4} surface are illustrated in Figure 3, and the charge differences are listed in the Supporting Information (Tables S2–S5). It is evident that there is no charge transfer during adsorption, as shown in Figure 3. In addition, the charge differences for all four

inhibitors were insignificant, indicating the physisorption mode of interaction. Consequently, the Bader analysis confirms no chemisorption interaction for adsorption energies ranging from -1.75 to -2.66 eV.

The top potential amino acid inhibitors are compared according to periodic DFT simulations, and quantum chemical calculations are given in Table 7. As per the binding energy calculations, the inhibition performance is predicted to be in the order tyrosine > phenylalanine > alanine > aspartic acid. However, the value of the adsorption energy of alanine (-2.16 eV) was close to that of phenylalanine (-2.24 eV). However, phenylalanine could have better inhibition efficiency because possessing a higher TNC translated into higher adsorption onto the calcite scale surface.⁵⁸ Furthermore, tyrosine has the highest TNC compared to the other amino acids, which could be the prime factor reflecting on its highest reported adsorption energy. Similarly, aspartic acid has features of a good inhibitor such as lowest X , ΔE_{Gap} , and ω .^{44,81} Nevertheless, the interaction energy simulations revealed the physical adsorption of low energy onto the calcite surface. Generally, adsorption energy ($E_{\text{adsorption}}$) is the key indicator of the inhibition efficiency; however, inhibitor molecules could also be distinguished by relying on some electronic structure parameters when there is no considerable difference in adsorption energy.

5. CONCLUSIONS

Oilfield scales form deposits on solid surfaces, and their impervious nature could reduce hydrocarbon productivity, leading to massive economic losses. Therefore, to ensure the sustainability of oil and gas wells, it is essential to understand the formation mechanism and prevention methods. Among the formed scales types, calcium carbonate scales are the most observed in the production facilities, with the amorphous state called calcite as their most stable form. Several chemicals that behave as scale inhibitors have been applied to retard solid surface formation, deposition, and growth. Phosphonate- and carboxylate-based inhibitors have successfully achieved high inhibition efficiency. However, due to strict environmental regulations, the research efforts are geared toward examining green scale inhibitors.

This paper investigated the performance of 10 amino acids classified as green inhibitors for calcite scales using molecular simulations. Initially, the eco-toxicity evaluation showed that all considered amino acids are safe from the aspects of

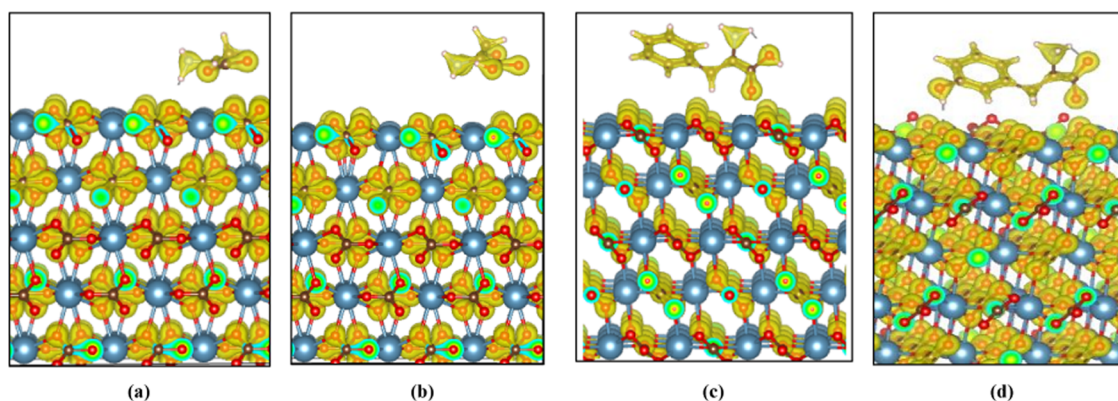
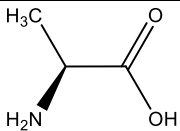
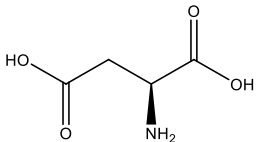
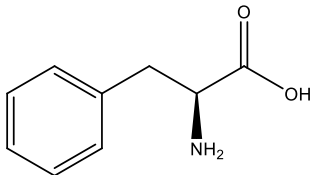
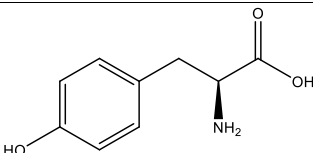


Figure 3. Bader charge densities of the calcite {1 0 4} surface with (a) alanine (on top), (b) aspartic acid (on top), (c) phenylalanine (on middle), and (d) tyrosine (on middle).

Table 7. Comparison of the Top Four Amino Acid Inhibitors as per the Periodic DFT Simulations and Quantum Chemical Calculations

Inhibitor	Chemical Structure	Mw (g/mol)	Solubility LogS	$E_{adsorption}$ (eV)	ΔE_{Gap} (eV)	X (eV)	ω (eV)	TNC (eV)
Alanine (on top)		89.09	1.54 (highly soluble)	-2.16	4.47	2.75	8.46	-2.44
Aspartic acid (on top)		133.10	1.98 (highly soluble)	-1.75	4.07	2.40	5.85	-3.40
Phenylalanine (on middle)		165.19	-0.08 (very soluble)	-2.24	4.55	2.82	9.03	-4.41
Tyrosine (on middle)		181.19	0.39 (highly soluble)	-2.66	4.59	2.83	9.17	-5.20

carcinogenicity, honey bee toxicity, crustacean, and aquatic fish toxicity. The DFT simulation and quantum chemical calculations revealed that alanine, aspartic acid, phenylalanine, and tyrosine amino acids are the top potential suitable inhibitors. After that, the periodic DFT simulations for studying the interaction with calcite predicted that the inhibition efficiency order is tyrosine > phenylalanine > alanine > aspartic acid. The calcite {1 0 4} surface was explored for potential adsorption sites that facilitate the interaction with the inhibitors, and optimum positions were determined. The weakest predicted calcite inhibition efficiency by aspartic acid is in agreement with some experimental studies, demonstrating that it is efficient only at very high concentrations. The geometrical structures along with Bader charge analysis confirmed the physisorption nature of all examined amino acid inhibitors with adsorption energies ranging from -1.75 to -2.66 eV. In sum, this theoretical study could guide real laboratory examinations based on the predicted performance from molecular simulations.

■ ASSOCIATED CONTENT

SI Supporting Information

The Supporting Information is available free of charge at <https://pubs.acs.org/doi/10.1021/acsomega.1c04888>.

Details of inhibitor-scale surface interaction energy for three different positions of each inhibitor on the calcite surface; and Bader charge before and after adsorption onto calcite (PDF)

■ AUTHOR INFORMATION

Corresponding Authors

Mohammed A. Saad – Gas Processing Center, College of Engineering, Qatar University, P.O. Box 2713 Doha, Qatar; Email: m.saleh@qu.edu.qa

Ibnelwaleed A. Hussein – Gas Processing Center, College of Engineering, Qatar University, P.O. Box 2713 Doha, Qatar; orcid.org/0000-0002-6672-8649; Phone: +974 4403 4370/7694; Email: ihussein@qu.edu.qa

Authors

Rem Jalab – Gas Processing Center, College of Engineering, Qatar University, P.O. Box 2713 Doha, Qatar

Abdulmujeeb T. Onawole – Gas Processing Center, College of Engineering, Qatar University, P.O. Box 2713 Doha, Qatar

Complete contact information is available at: <https://pubs.acs.org/doi/10.1021/acsomega.1c04888>

Notes

The authors declare no competing financial interest.

■ ACKNOWLEDGMENTS

This publication was made possible by Qatar University Grant No. QUCP-CENG-2021-3. The statements made herein are solely the responsibility of the authors. Gas Processing Center at Qatar University is acknowledged for providing the support and facilities. In addition, the authors would like to acknowledge the use of computational resources provided by Texas A&M University in Qatar.

REFERENCES

- (1) Kumar, S.; Naiya, T. K.; Kumar, T. Developments in Oilfield Scale Handling towards Green Technology-A Review. *J. Pet. Sci. Eng.* **2018**, *169*, 428–444.
- (2) Macadam, J.; Parsons, S. A. Calcium Carbonate Scale Control, Effect of Material and Inhibitors. *Water Sci. Technol.* **2004**, *49*, 153–159.
- (3) Antony, A.; Low, J. H.; Gray, S.; Childress, A. E.; Le-Clech, P.; Leslie, G. Scale Formation and Control in High Pressure Membrane Water Treatment Systems: A Review. *J. Membr. Sci.* **2011**, *383*, 1–16.
- (4) Baraka-Lokmane, S.; Sorbie, K.; Poisson, N.; Kohler, N. Can Green Scale Inhibitors Replace Phosphonate Scale Inhibitors?: Carbonate Coreflooding Experiments. *Pet. Sci. Technol.* **2009**, *27*, 427–441.
- (5) Al-Roomi, Y. M.; Hussain, K. F. Potential Kinetic Model for Scaling and Scale Inhibition Mechanism. *Desalination* **2016**, *393*, 186–195.
- (6) Senthilmurugan, B.; Ghosh, B.; Sanker, S. High Performance Maleic Acid Based Oil Well Scale Inhibitors-Development and Comparative Evaluation. *J. Ind. Eng. Chem.* **2011**, *17*, 415–420.
- (7) Lee, S.; Lee, C. H. Effect of Operating Conditions on CaSO₄ Scale Formation Mechanism in Nanofiltration for Water Softening. *Water Res.* **2000**, *34*, 3854–3866.
- (8) Hamdy, E.; Bakr, M. A.; Hay, A. A.; Sisostris, S.; Anwar, M.; El Farouk, O. In *Challenge and Successful Application for Scale Removal in Oil Field, Egypt: Field Study*, Soc. Pet. Eng. - Int. Pet. Technol. Conf. 2014, IPTC 2014 - Innov. Collab. Keys to Afford. Energy, 2014; pp 3610–3616.
- (9) Li, J.; Tang, M.; Ye, Z.; Chen, L.; Zhou, Y. Scale Formation and Control in Oil and Gas Fields: A Review. *J. Dispers. Sci. Technol.* **2017**, *38*, 661–670.
- (10) Kamal, M. S.; Hussein, I.; Mahmoud, M.; Sultan, A. S.; Saad, M. A. S. Oilfield Scale Formation and Chemical Removal: A Review. *J. Pet. Sci. Eng.* **2018**, *171*, 127–139.
- (11) Lakshmi, D. S.; Senthilmurugan, B.; Drioli, E.; Figoli, A. Application of Ionic Liquid Polymeric Microsphere in Oil Field Scale Control Process. *J. Pet. Sci. Eng.* **2013**, *112*, 69–77.
- (12) Helalizadeh, A.; Müller-Steinhagen, H.; Jamialahmadi, M. Mixed Salt Crystallisation Fouling. *Chem. Eng. Process.* **2000**, *39*, 29–43.
- (13) Moghadasi, J.; Jamialahmadi, M.; Müller-Steinhagen, H.; Sharif, A. In *Formation Damage Due to Scale Formation in Porous Media Resulting From Water Injection*, SPE International Symposium and Exhibition on Formation Damage Control, Louisiana, USA, 2004; pp 1–11.
- (14) Kiaei, Z.; Haghtalab, A. Experimental Study of Using Ca-DTPMP Nanoparticles in Inhibition of CaCO₃ Scaling in a Bulk Water Process. *Desalination* **2014**, *338*, 84–92.
- (15) Mpelwa, M.; Tang, S. F. State of the Art of Synthetic Threshold Scale Inhibitors for Mineral Scaling in the Petroleum Industry: A Review. *Pet. Sci.* **2019**, *16*, 830–849.
- (16) Farooqui, N. M.; Sorbie, K. S.; Boak, L. S. In *Molecular Weight Effects in Polymeric Scale Inhibitor Precipitation Squeeze Treatments*, SPE -European Formation Damage Conference and Exhibition, Budapest, Hungary, 2015; pp 843–857.
- (17) Wang, Q.; Liang, F.; Al-Nasser, W.; Al-Dawood, F.; Al-Shafai, T.; Al-Badair, H.; Shen, S.; Al-Ajwad, H. Laboratory Study on Efficiency of Three Calcium Carbonate Scale Inhibitors in the Presence of EOR Chemicals. *Petroleum* **2018**, *4*, 375–384.
- (18) Harouaka, K.; Kan, A. T.; Tomson, M. Calcite Deposition Kinetics and the Effect of Phosphonate and Carboxylate Inhibitors at 150 °C. *Appl. Geochem.* **2019**, *109*, No. 104393.
- (19) Issabayev, Y. A.; Boiko, G. I.; Lyubchenko, N. P.; Shaikhutdinov, Y. M.; et al. Synthesis of Unexplored Aminophosphonic Acid and Evaluation as Scale Inhibitor for Industrial Water Applications. *J. Water Process Eng.* **2018**, *22*, 192–202.
- (20) Zhang, P.; Shen, D.; Ruan, G.; Kan, A. T.; Tomson, M. B. Phosphino-Polycarboxylic Acid Modified Inhibitor Nanomaterial for Oilfield Scale Control: Synthesis, Characterization and Migration. *J. Ind. Eng. Chem.* **2017**, *45*, 366–374.
- (21) Sanni, O. S.; Bukuaghangin, O.; Charpentier, T. V. J.; Neville, A. Evaluation of Laboratory Techniques for Assessing Scale Inhibition Efficiency. *J. Pet. Sci. Eng.* **2019**, *182*, No. 106347.
- (22) Mady, M. F.; Malmin, H.; Kelland, M. A. Sulfonated Nonpolymeric Aminophosphonate Scale Inhibitors- Improving the Compatibility and Biodegradability. *Energy Fuels* **2019**, *33*, 6197–6204.
- (23) Asghari, E.; Gholizadeh-khajeh, M.; Ashassi-sorkhabi, H. Tartaric Acid as a Non-Toxic and Environmentally-Friendly Anti-Scaling Material for Using in Cooling Water Systems: Electrochemical and Surface Studies. *J. Mater. Eng. Perform.* **2016**, *25*, 4230–4238.
- (24) Karar, A.; Naamoune, F. Inhibition of Calcium Carbonate Precipitation by Citric Acid. *Mater. Biomater. Sci.* **2018**, *01*, 019–023.
- (25) Štajner, L.; Kontrec, J.; Njegić Džakula, B.; Maltar-Strmečki, N.; Plodinec, M.; Lyons, D. M.; Kralj, D. The Effect of Different Amino Acids on Spontaneous Precipitation of Calcium Carbonate Polymorphs. *J. Cryst. Growth* **2018**, *486*, 71–81.
- (26) Jafar Mazumder, M. A. A Review of Green Scale Inhibitors: Process, Types, Mechanism and Properties. *Coatings* **2020**, *10*, No. 928.
- (27) Wedenig, M.; Boch, R.; Leis, A.; Wagner, H.; Dietzel, M. Green Inhibitor Performance against CaCO₃ Scaling: Rate-Modeling Aided Test Procedure. *Cryst. Growth Des.* **2021**, *21*, 1959–1971.
- (28) Abd-El-nabey, B. A.; Abd-El-khalek, D. E.; El-Housseiny, S.; Mohamed, M. E. Plant Extracts as Corrosion and Scale Inhibitors: A Review. *Int. J. Corros. Scale Inhib.* **2020**, *9*, 1287–1328.
- (29) Hajizadeh, A.; Lotfabad, T. B.; Bahmaei, M. Assessment of Aqueous Extract of Gypsophila Aretioides for Inhibitory Effects on Calcium Carbonate Formation. *Green Process. Synth.* **2019**, *8*, 464–473.
- (30) Vasyliov, G.; Vorobyova, V.; Zhuk, T. Raphanus Sativus L. Extract as a Scale and Corrosion Inhibitor for Mild Steel in Tap Water. *J. Chem.* **2020**, *2020*, No. 5089758.
- (31) Popov, K. I.; Kovaleva, N. E.; Rudakova, G. Y.; Kombarova, S. P.; Larchenko, V. E. Recent State-of-the-Art of Biodegradable Scale Inhibitors for Cooling-Water Treatment Applications (Review). *Therm. Eng.* **2016**, *63*, 122–129.
- (32) Chaussemier, M.; Pourmohtasham, E.; Gelus, D.; Pécou, N.; Perrot, H.; Lédion, J.; Cheap-Charpentier, H.; Horner, O. State of Art of Natural Inhibitors of Calcium Carbonate Scaling. A Review Article. *Desalination* **2015**, *356*, 47–55.
- (33) Sun, Y.; Xiang, W.; Wang, Y. Study on Polyepoxysuccinic Acid Reverse Osmosis Scale Inhibitor. *J. Environ. Sci.* **2009**, *21*, S73–S75.
- (34) Yan, M.; Tan, Q.; Liu, Z.; Li, H.; Zheng, Y.; Zhang, L.; Liu, Z. Synthesis and Application of a Phosphorous-Free and Non-Nitrogen Polymer as an Environmentally Friendly Scale Inhibition and Dispersion Agent in Simulated Cooling Water Systems. *ACS Omega* **2020**, *5*, 15487–15494.
- (35) Chen, J.; Xu, L.; Han, J.; Su, M.; Wu, Q. Synthesis of Modified Polyaspartic Acid and Evaluation of Its Scale Inhibition and Dispersion Capacity. *Desalination* **2015**, *358*, 42–48.
- (36) Zhang, S.; Qu, H.; Yang, Z.; Fu, C.; Tian, Z.; Yang, W. Scale Inhibition Performance and Mechanism of Sulfamic/Amino Acids Modified Polyaspartic Acid against Calcium Sulfate. *Desalination* **2017**, *419*, 152–159.
- (37) Zeng, Y. W.; Ma, D. K.; Wang, W.; Chen, J. J.; Zhou, L.; Zheng, Y. Z.; Yu, K.; Huang, S. M. N, S Co-Doped Carbon Dots with Orange Luminescence Synthesized through Polymerization and Carbonization Reaction of Amino Acids. *Appl. Surf. Sci.* **2015**, *342*, 136–143.
- (38) Zhang, Y.; Zhang, S.; Tan, B.; Guo, L.; Li, H. Solvothermal Synthesis of Functionalized Carbon Dots from Amino Acid as an Eco-Friendly Corrosion Inhibitor for Copper in Sulfuric Acid Solution. *J. Colloid Interface Sci.* **2021**, *604*, 1–14.
- (39) Raghavendra, N.; Chitnis, S. R.; Sheelimath, D. S. Anti-Corrosion Investigation of Polylysine (Amino Acid Polymer) as Efficacious Corrosion Inhibitor for Al in Industrial Acidic Pickling Environment. *J. Bio-Tribo-Corros.* **2021**, *7*, No. 29.

- (40) Barouni, K.; Kassale, A.; Albourine, A.; Jbara, O.; Hammouti, B.; Bazzi, L. Amino Acids as Corrosion Inhibitors for Copper in Nitric Acid Medium: Experimental and Theoretical Study. *J. Mater. Environ. Sci.* **2014**, *5*, 456–463.
- (41) Zhang, Z.; Li, W.; Zhang, W.; Huang, X.; Ruan, L.; Wu, L. Experimental, Quantum Chemical Calculations and Molecular Dynamics (MD) Simulation Studies of Methionine and Valine as Corrosion Inhibitors on Carbon Steel in Phase Change Materials (PCMs) Solution. *J. Mol. Liq.* **2018**, *272*, 528–538.
- (42) Srivastava, V.; Haque, J.; Verma, C.; Singh, P.; Lgaz, H.; Salghi, R.; Quraishi, M. A. Amino Acid Based Imidazolium Zwitterions as Novel and Green Corrosion Inhibitors for Mild Steel: Experimental, DFT and MD Studies. *J. Mol. Liq.* **2017**, *244*, 340–352.
- (43) Hinsien, K. The Molecular Modeling Toolkit: A New Approach to Molecular Simulations. *J. Comput. Chem.* **2000**, *21*, 79–85.
- (44) Kaya, S.; Tüzün, B.; Kaya, C.; Obot, I. B. Determination of Corrosion Inhibition Effects of Amino Acids: Quantum Chemical and Molecular Dynamic Simulation Study. *J. Taiwan Inst. Chem. Eng.* **2016**, *58*, 528–535.
- (45) Umar, B. A.; Uzairu, A.; Shallangwa, G. A. Quantum Modeling and Molecular Dynamic Simulation of Some Amino Acids and Related Compounds on Their Corrosion Inhibition of Steel in Acidic Media. *Port. Electrochim. Acta* **2020**, *38*, 313–329.
- (46) Zhao, H.; Zhang, X.; Ji, L.; Hu, H.; Li, Q. Quantitative Structure-Activity Relationship Model for Amino Acids as Corrosion Inhibitors Based on the Support Vector Machine and Molecular Design. *Corros. Sci.* **2014**, *83*, 261–271.
- (47) Yang, M.; Mark Rodger, P.; Harding, J. H.; Stipp, S. L. S. Molecular Dynamics Simulations of Peptides on Calcite Surface. *Mol. Simul.* **2009**, *35*, 547–553.
- (48) Asthagiri, A.; Hazen, R. M. An Ab Initio Study of Adsorption of Alanine on the Chiral Calcite Surface. *Mol. Simul.* **2007**, *33*, 343–351.
- (49) ACD/Labs, *Advanced Chemistry Development (ACD/Labs) Software*.
- (50) Frisch, M. J.; Trucks, G. W.; Schlegel, H. B.; Scuseria, G. E.; Robb, M. A.; Cheeseman, J. R.; Scalmani, G.; Barone, V.; Mennucci, B.; Petersson, G. A.; Nakatsuji, H.; Caricato, M.; Li, X.; Hratchian, H. P.; Izmaylov, A. F.; Bloino, J.; Zheng, G.; Sonnenberg, J. L.; Hada, M.; Ehara, M.; Toyota, K.; Fukuda, R.; Hasegawa, J.; Ishida, M.; Nakajima, T.; Honda, Y.; Kitao, O.; Nakai, H.; Vreven, T.; Montgomery, J. A. J.; Peralta, J. E.; Ogliaro, F.; Bearpark, M.; Heyd, J. J.; Brothers, E.; Kudin, K. N.; Staroverov, V. N.; Kobayashi, R.; Normand, J.; Raghavachari, K.; Rendell, A.; Burant, J. C.; Iyengar, S. S.; Tomasi, J.; Cossi, M.; Rega, N.; Millam, J. M.; Klene, M.; Knox, J. E.; Cross, J. B.; Bakken, V.; Adamo, C.; Jaramillo, J.; Gomperts, R.; Stratmann, R. E.; Yazyev, O.; Austin, A. J.; Cammi, R.; Pomelli, C.; Ochterski, J. W.; Martin, R. L.; Morokuma, K.; Zakrzewski, V. G.; Voth, G. A.; Salvador, P.; Dannenberg, J. J.; Dapprich, S.; Daniels, A. D.; Farkas, Ö.; Foresman, J. B.; Ortiz, J. V.; Cioslowski, J.; Fox, D. J. *Gaussian 09*, revision D.01; Gaussian, Inc.: Wallingford CT. <https://doi.org/10.1063/PT.4.2023>, 2013.
- (51) Obot, I. B. B.; Macdonald, D. D. D.; Gasem, Z. M. M. Density Functional Theory (DFT) as a Powerful Tool for Designing New Organic Corrosion Inhibitors: Part I: An Overview. *Corros. Sci.* **2015**, *99*, 1–30.
- (52) Umoren, S. A.; Solomon, M. M.; Madhankumar, A.; Obot, I. B. Exploration of Natural Polymers for Use as Green Corrosion Inhibitors for AZ31 Magnesium Alloy in Saline Environment. *Carbohydr. Polym.* **2020**, *230*, No. 115466.
- (53) Sulaiman, K. O.; Onawole, A. T.; Faye, O.; Shuaib, D. T. Understanding the Corrosion Inhibition of Mild Steel by Selected Green Compounds Using Chemical Quantum Based Assessments and Molecular Dynamics Simulations. *J. Mol. Liq.* **2019**, *279*, 342.
- (54) Kruse, H.; Goerigk, L.; Grimme, S. Why the Standard B3LYP/6-31G* Model Chemistry Should Not Be Used in DFT Calculations of Molecular Thermochemistry: Understanding and Correcting the Problem. *J. Org. Chem.* **2012**, *77*, 10824–10834.
- (55) Tomasi, J.; Mennucci, B.; Cammi, R. Quantum Mechanical Continuum Solvation Models. *Chem. Rev.* **2005**, *105*, 2999–3093.
- (56) Tsuneda, T.; Song, J. W.; Suzuki, S.; Hirao, K. On Koopmans' Theorem in Density Functional Theory. *J. Chem. Phys.* **2010**, *133*, No. 174101.
- (57) Koopmans, T. Ordering of Wave Functions and Eigen Energies to the Individual Electrons of an Atom. *Physica* **1934**, *1*, 104–113.
- (58) El Adnani, Z.; Mcharfi, M.; Sfaira, M.; Benzakour, M.; Benjelloun, A. T.; Ebn Touhami, M. DFT Theoretical Study of 7-R-3methylquinoxalin-2(1H)-Thiones (RH; CH3; Cl) as Corrosion Inhibitors in Hydrochloric Acid. *Corros. Sci.* **2013**, *68*, 223–230.
- (59) Udhayakala, P.; Rajendiran, T. V.; Gunasekaran, S. Quantum Chemical Investigations on Some Quinoxaline Derivatives as Effective Corrosion Inhibitors for Mild Steel. *Der Pharm. Lett.* **2012**, *4*, 1285–1298.
- (60) Mulliken, R. S. Electronic Population Analysis on LCAO-MO Molecular Wave Functions. I. *J. Chem. Phys.* **1955**, *23*, 1833–1840.
- (61) Kresse, G.; Joubert, D. From Ultrasoft Pseudopotentials to the Projector Augmented-Wave Method. *Phys. Rev. B* **1999**, *59*, 1758–1775.
- (62) Yang, L. M.; Ganz, E.; Svelle, S.; Tilset, M. Computational Exploration of Newly Synthesized Zirconium Metal-Organic Frameworks UiO-66, -67, -68 and Analogues. *J. Mater. Chem. C* **2014**, *2*, 7111–7125.
- (63) Perdew, J. P.; Burke, K.; Ernzerhof, M. Generalized Gradient Approximation Made Simple. *Phys. Rev. Lett.* **1996**, *77*, No. 3865.
- (64) Toulhoat, H.; Raybaud, P.; Kasztelan, S.; Kresse, G.; Hafner, J. Transition Metals to Sulfur Binding Energies Relationship to Catalytic Activities in HDS: Back to Sabatier with First Principle Calculations. *Catal. Today* **1999**, *50*, 629–636.
- (65) Blöchl, P. E. Generalized Separable Potentials for Electronic-Structure Calculations. *Phys. Rev. B* **1990**, *41*, No. 5414.
- (66) Davis, J. B. A.; Baletto, F.; Johnston, R. L. The Effect of Dispersion Correction on the Adsorption of CO on Metallic Nanoparticles. *J. Phys. Chem. A* **2015**, *119*, 9703.
- (67) Grimme, S.; Antony, J.; Ehrlich, S.; Krieg, H. A Consistent and Accurate Ab Initio Parametrization of Density Functional Dispersion Correction (DFT-D) for the 94 Elements H-Pu. *J. Chem. Phys.* **2010**, *132*, No. 154104.
- (68) *Materials Studio Dassault Syst'emes BIOVIA*; Dassault Syst'emes: San Diego, California, 2017.
- (69) Carchini, G.; Hussein, I.; Al-Marri, M. J.; Shawabkeh, R.; Mahmoud, M.; Aparicio, S. A Theoretical Study of Gas Adsorption on Calcite for CO₂ Enhanced Natural Gas Recovery. *Appl. Surf. Sci.* **2019**, *504*, No. 144575.
- (70) Kratzer, P.; Neugebauer, J. The Basics of Electronic Structure Theory for Periodic Systems. *Front. Chem.* **2019**, *7*, No. 106.
- (71) Smidstrup, S.; Markussen, T.; Vancaerfeld, P.; Wellendorff, J.; Schneider, J.; Gunst, T.; Verstichel, B.; Stradi, D.; Khomyakov, P. A.; Vej-Hansen, U. G.; Lee, M. E.; Chill, S. T.; Rasmussen, F.; Penazzi, G.; Corsetti, F.; Ojanperä, A.; Jensen, K.; Palsgaard, M. L. N.; Martinez, U.; Blom, A.; Brandbyge, M.; Stokbro, K. QuantumATK: An Integrated Platform of Electronic and Atomic-Scale Modelling Tools. *J. Phys. Condens. Matter* **2020**, *32*, No. 015901.
- (72) Onawole, A. T.; Hussein, I. A.; Ahmed, M. E. M.; Saad, M. A.; Aparicio, S. Ab Initio Molecular Dynamics of the Dissolution of Oilfield Pyrite Scale Using Borax. *J. Mol. Liq.* **2020**, *302*, No. 112500.
- (73) Dassault Systèmes, *BIOVIA Materials Studio*, San Diego, 2017.
- (74) Yang, H.; Cai, Y.; Lou, C.; Tang, Y.; Wang, Z.; Liu, G.; Li, W.; Sun, L.; Li, J. AdmetSAR 2.0: Web-Service for Prediction and Optimization of Chemical ADMET Properties. *Bioinformatics* **2019**, *35*, 1067–1069.
- (75) Yang, H.; Sun, L.; Wang, Z.; Li, W.; Liu, G.; Tang, Y. ADMETopt: A Web Server for ADMET Optimization in Drug Design via Scaffold Hopping. *J. Chem. Inf. Model.* **2018**, *58*, 2051–2056.
- (76) Daina, A.; Michielin, O.; Zoete, V. SwissADME: A Free Web Tool to Evaluate Pharmacokinetics, Drug-Likeness and Medicinal Chemistry Friendliness of Small Molecules. *Sci. Rep.* **2017**, *7*, No. 42717.

(77) SwissADME. <http://swissadme.ch/index.php> (accessed May 1, 2021).

(78) Delaney, J. S. ESOL: Estimating Aqueous Solubility Directly from Molecular Structure. *J. Chem. Inf. Comput. Sci.* **2004**, *44*, 1000–1005.

(79) Ritchie, T. J.; MacDonald, S. J. F.; Young, R. J.; Pickett, S. D. The Impact of Aromatic Ring Count on Compound Developability: Further Insights by Examining Carbo- and Hetero-Aromatic and -Aliphatic Ring Types. *Drug Discovery Today* **2011**, *16*, 164–171.

(80) Sulaiman, K. O.; Onawole, A. T. Quantum Chemical Evaluation of the Corrosion Inhibition of Novel Aromatic Hydrazide Derivatives on Mild Steel in Hydrochloric Acid. *Comput. Theor. Chem.* **2016**, *1093*, 73–80.

(81) Parr, R. G.; Szentpály, L. V.; Liu, S. Electrophilicity Index. *J. Am. Chem. Soc.* **1999**, *121*, 1922–1924.

(82) Hamdona, S. K.; Hamza, S. M.; Mangood, A. H. Effect of Some Amino Acids on the Rate of Dissolution of Calcite Crystals in Aqueous Systems. *Desalination* **1995**, *101*, 263–267.

(83) Barouni, K.; Kassale, A.; Bazzi, L.; Salghi, R.; Hammouti, B.; Albourine, A.; El Issami, S.; Jbara, O.; Bouachrine, M. Inhibition of Corrosion of Copper in Nitric Acid Solution by Four Amino Acids. *Res. Chem. Intermed.* **2014**, *40*, 991–1002.

(84) Ji, Y.; Chen, Y.; Le, J.; Qian, M.; Huan, Y.; Yang, W.; Yin, X.; Liu, Y.; Wang, X.; Chen, Y. Highly Effective Scale Inhibition Performance of Amino Trimethylenephosphonic Acid on Calcium Carbonate. *Desalination* **2017**, *422*, 165–173.